Shannon entropy and avoided crossings in closed and open quantum billiards

Kyu-Won Park,[1] Songky Moon,[1] Younghoon Shin,[1] Jinuk Kim,[1] Kabgyun Jeong,[2] and Kyungwon An[1,*]
[1]*School of Physics and Astronomy, Seoul National University, Seoul 08826, Korea*
[2]*IMDARC, Department of Mathematical Sciences, Seoul National University, Seoul 08826, Korea*

(Received 25 November 2017; published 12 June 2018)

The relation between Shannon entropy and avoided crossings is investigated in dielectric microcavities. The Shannon entropy of the probability density for eigenfunctions in an open elliptic billiard as well as a closed quadrupole billiard increases as the center of the avoided crossing is approached. These results are opposite to those of atomic physics for electrons. It is found that the collective Lamb shift of the open quantum system and the symmetry breaking in the closed chaotic quantum system have equivalent effects on the Shannon entropy.

DOI: 10.1103/PhysRevE.97.062205

I. INTRODUCTION

Shannon entropy, first introduced by Shannon in communication theory [1], is a relevant measure of the average amount of information for a random variable with a specific probability distribution function. Shannon entropy is generally equivalent to von Neumann entropy for a physical observable with eigenvalues or probability densities. Not only is it useful in modern information theory, but it also has important applications in quantum physics related to the uncertainty principle [2,3] and quantum measurement [4,5] as well as in other areas. Shannon entropy has been applied to the identification of putative drug targets in a biosystem [6] and descriptor analysis for distinguishing natural products from synthetic molecules [7], and it was also used to measure topological diversity related to economics [8] and to detect defects in acoustic emission [9]. Recently, Shannon entropy has also been used as an indicator for avoided crossing in atomic systems [10,11].

Avoided crossing is a phenomenon in which the two eigenvalues of a Hamiltonian come close and then repel each other as a system parameter is varied. It signifies the presence of an interaction between states in the Hamiltonian. For this reason, the avoided crossing has been a fundamentally important concept [12] from the beginning of quantum mechanics. It has been extensively studied theoretically as well as experimentally in various physical systems [13–16]. Especially in the fields of molecular systems, the relation between avoided crossing and the onset of chaos was investigated [17,18]. For convenience of distinction, avoided crossings in conservative or closed systems are called avoided level crossings (ALCs), whereas avoided resonance crossings (ARCs) are their extension to open or dissipative systems [19]. For strong coupling, both cases show similar behaviors but may have different physical origins for avoided crossings. In particular, ALCs in closed quantum billiards are due to the symmetry breaking in a block diagonal matrix [20,21], while ARCs can be due to the openness effects [22–25]. Especially, integrable systems such as an ellipse or a rectangle can be an interesting platform for studying ARCs since the openness effects are the sole source [22,24] of avoided crossings. The avoided crossings in quantum billiards have been investigated in relation to exceptional points [26–31], unidirectional emission [32], dynamical tunneling [33], high-quality factors [34], ray dynamics [35], and so on. However, Shannon entropy, despite its utility, has not been applied to the avoided crossings in quantum billiards to the best of our knowledge.

In this paper, we investigated the relation between Shannon entropy and avoided crossings under strong coupling in dielectric microcavities. We then found that Shannon entropy increases due to coherent superposition of wave functions as the center of the avoided crossing is approached. This result is opposite to the previous one obtained for electrons in atomic systems [10,11], where Shannon entropy decreases due to electron ionization as we move close to the center of the avoided crossing. In addition, we compared the openness effects and the chaotic effects on Shannon entropy. For this, we adopted an elliptic billiard as an integrable system for manifesting the openness effects [24] and a quadrupole billiard [36] as a nonintegrable system for manifesting chaotic effects, respectively.

This paper is organized as follows. In Sec. II, we compare an open quantum system and a closed chaotic quantum system. In Sec. III, we study Shannon entropy for closed and open elliptic billiards. Shannon entropy for a closed quadrupole billiard is presented in Sec. IV. Maximal entropy states and the effects of the self-energy Lamb shift to Shannon entropy are discussed in Sec. V. Finally, we summarize our work in Sec. VI.

II. COMPARISON BETWEEN AN OPEN QUANTUM SYSTEM AND A CLOSED CHAOTIC QUANTUM SYSTEM

The avoided crossing takes place when the off-diagonal terms of the Hamiltonian become prominent. These off-diagonal terms arise from various sources depending on the properties of each system. First, let us briefly recapitulate the avoided crossings due to the openness effects. These openness effects are well described by a non-Hermitian Hamiltonian, first developed in nuclear physics [37] and then applied to other areas such as atomic physics [38], microwave cavities

*kwan@phya.snu.ac.kr

[39], solid-state physics [40], dielectric microcavities [24,41], and so on.

The non-Hermitian Hamiltonian for an open quantum system can be obtained by introducing the Feshbach projective operator π_S and π_B with $\pi_S\pi_B = \pi_B\pi_S = 0$ and $\pi_S + \pi_S = I_T$. Here, π_S is a projective operator onto a closed quantum system and π_B is a projective operator onto a bath, respectively. The operator I_T is an identity operator for the total system-bath space. With these operators and the Hamiltonian for the total system-bath space H_T, we define useful operators such as $H_S = \pi_S H_T \pi_S$, $H_B = \pi_B H_T \pi_B$, $V_{SB} = \pi_S H_T \pi_B$, and $V_{BS} = \pi_B H_T \pi_S$, where H_S (H_B) is a Hamiltonian of the closed quantum system (bath). V_{SB} denotes an interaction from the bath to the closed quantum system, and V_{BS} denotes the opposite [22,23]. The non-Hermitian Hamiltonian is then defined as

$$H_{\text{eff}} = H_S + V_{SB} G_B^+ V_{BS}, \tag{1}$$

with an outgoing Green function G_B^+ in a bath. The Green function is defined as $G_B^+ \equiv (\mu^+ - H_B)^{-1}$, where μ^+ is an eigenvalue of H_B with a small positive imaginary number added for outgoing states: $\mu^+ \equiv \mu + i\eta$ and $\lim_{\eta\to 0^+}$. If H_S with eigenvalue ϵ_j for the jth eigenstate $|\epsilon_j\rangle$ describes an integrable system (no internal interaction), only the second term, $V_{SB} G_B^+ V_{BS}$, can lead to avoided crossings. In this case, the outgoing Green function plays a crucial role in the system-bath interaction. That is, the G_B^+ can route the state not only to the same state but also to a different state $|\epsilon_j\rangle \neq |\epsilon_k\rangle$, resulting in the collective Lamb shift, otherwise it is the self-energy Lamb shift. Thus, this interaction via the bath (the collective Lamb shift) can induce an avoided crossing as well as a coherent superposition of wave functions [42]. On the other hand, the interaction with the bath itself is just giving rise to mode decay [24], not the avoided crossings.

There are several well-known topics related to chaotic effects such as scar formation [43], Anderson localization [44], trace formula [45], and so on. But here we would rather focus on the structure of the Hamiltonian itself to deal with avoided crossing. So, let us recapitulate the Hamiltonian properties for a closed chaotic system. The energy repulsions in quantum chaos are well explained by the random matrix theory [20,21,46,47]. When there are n-quantum numbers $(O^1, O^2, \ldots, O^n)$ in a system with n-degrees of freedom, the system is integrable. If not, it is chaotic. This property is fundamentally related to symmetries in the system. That is, if we can find $(n-1)$ observables that commute with Hamiltonian H, i.e., $[H, O^i] = 0$, giving a complete basis set $|O^1, \ldots, O^n\rangle$, then the Hamiltonian H is fully diagonal with respect to this complete basis set. If not, the Hamiltonian is block-diagonal, having off-diagonal terms. When the symmetries are broken, the size of the block-diagonal matrix increases with the number of blocks decreasing.

III. COMPARISON BETWEEN SHANNON ENTROPIES IN CLOSED AND OPEN ELLIPTIC BILLIARDS

Let us consider a closed elliptic microcavity with a major axis a and a minor axis b. We are interested in its eigenvalues λ_k and eigenfunctions $\psi^{\text{ce}}(\mathbf{r})$:

$$H^{\text{ce}}\psi_k^{\text{ce}}(\mathbf{r}) = \lambda_k \psi_k^{\text{ce}}(\mathbf{r}), \tag{2}$$

where the superscript "ce" stands for a closed elliptic billiard with Dirichlet condition $\psi(\mathbf{r} = \mathcal{R}) = 0$ along the boundary. Here $\mathbf{r}$ is a two-dimensional position vector, and $\mathcal{R}$ represents the boundary of the billiard. We consider transverse-magnetic (TM) modes only with $\psi(\mathbf{r})$ corresponding to the electric field. The eigenvalues are calculated by using the boundary element method (BEM) [48] with a scanning parameter χ for $a = 1 + \chi$ and $b = \frac{1}{1+\chi}$ (constant area). In Fig. 1(a), the real part kR of the eigenvalues is plotted as the eccentricity $e \equiv \sqrt{1 - (\frac{b}{a})^2}$ is varied from 0.765 to 0.855 with an interval $\Delta\chi = 10^{-5}$. The intensities of some of the corresponding eigenfunctions are also shown. A mode crossing is observed near $e \simeq 0.805$, and their eigenfunctions are almost unchanged across the mode crossing. This behavior is well known and expected from the random matrix theory. The closed elliptic billiard is an integrable system, and thus it cannot lead to avoided crossings, resulting in Poisson distributions [20,21,46,47]. However, it was reported that the closed elliptic billiard may lead to Demkov-type interaction in some cases [49]. The Demkov-type avoided crossing occurs over a broad range between two eigenfunctions giving rise to a new pair of eigenfunctions localized on periodic orbits. In contrast, the usual Landau-Zener-type avoided crossing occurs over a short range between two eigenfunctions with exchange of their characteristics.

Next, let us consider an open elliptic cavity with complex eigenvalues z_k and their eigenfunctions $\psi_k^{\text{oe}}(\mathbf{r})$ of the non-Hermitian Hamiltonian H^{oe}, where the superscript "oe" indicates an open elliptic billiard with boundary conditions $\psi_{\text{in}}(\mathbf{r} = \mathcal{R}) = \psi_{\text{out}}(\mathbf{r} = \mathcal{R})$ and $\partial_n\psi_{\text{in}}(\mathbf{r} = \mathcal{R}) = \partial_n\psi_{\text{out}}(\mathbf{r} = \mathcal{R})$ for the TM mode. For a fair comparison with the closed elliptic cavity, we also consider TM modes for the open elliptic cavity. The Hamiltonian H^{oe} can be expressed as [22,23]

$$H^{\text{oe}} = H^{\text{ce}} + V_{SB} G_B^+ V_{BS} \tag{3}$$

similar to Eq. (1), exhibiting non-Hermitian properties such as $H^{\text{oe}} \neq (H^{\text{oe}})^\dagger$.

In Fig. 1(b), the real part kR of its eigenvalues z_k and the intensities of some of the eigenfunctions $\psi_k^{\text{oe}}(\mathbf{r})$ are plotted as the eccentricity is varied. An avoided crossing takes place near $e = e_c \cong 0.81$. The eigenfunctions corresponding to G and J are mixed at the center of the avoided crossing (H and K), and then exchanged at I and L. Moreover, the probability distributions (intensity plots) of the mixed eigenfunctions at H and K show more uniform patterns than the unmixed ones at G, J, I, and L. We will use Shannon entropy to quantify the degree of uniformity.

For a given discrete probability distribution $\rho(r_i)$ and N number of states, Shannon entropy is defined as

$$S(\rho(r_i)) \equiv -\sum_{i=1}^{N} \rho(r_i) \log \rho(r_i), \tag{4}$$

where $\sum_{i=1}^{N} \rho(r_i) = 1$. We apply this definition to the probability density for a closed elliptic billiard $S(\rho_k^{\text{ce}}(r_i))$ with a normalization condition $\sum_{i=1}^{N} \rho_k^{\text{ce}}(r_i) = \sum_{i=1}^{N} |\psi_k^{\text{ce}}(\mathbf{r})|^2 = 1$ for N states or mesh points. We also define a relative deformation parameter χ_e for the avoided crossing as

$$\chi_e = \frac{e - e_c}{e} \tag{5}$$

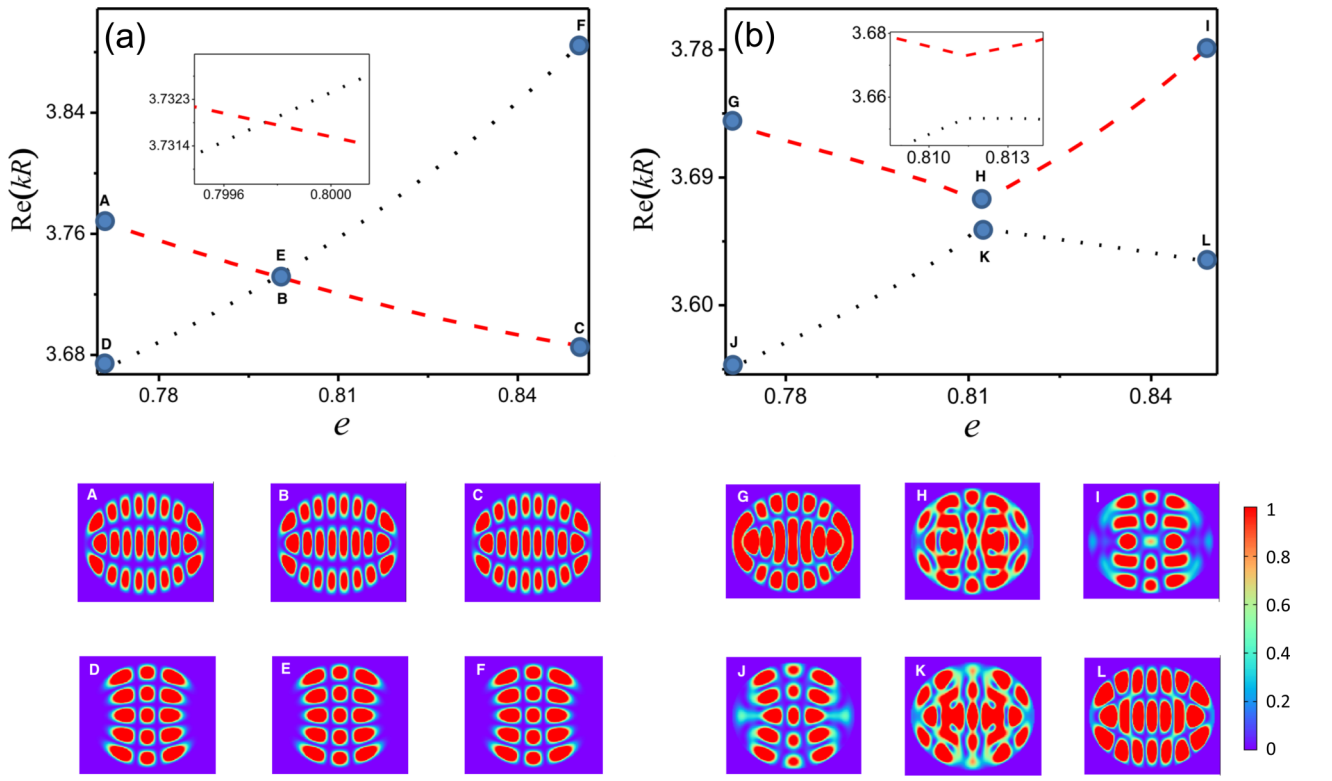

FIG. 1. (a) The real part kR of eigenvalues with their magnified view (inset) near the mode crossing and the intensities of some representative eigenfunctions for a closed elliptic microcavity with the eccentricity e. The eigenvalues show a mode crossing near $e \simeq 0.805$ and their eigenfunctions are almost unchanged across the mode crossing. (b) The real part kR of the eigenvalues with their magnified view (inset) near the center of the avoided crossing and the intensities of some representative eigenfunctions for an open elliptic microcavity as a function of the eccentricity. The avoided crossing takes place near $e \simeq 0.81$ and the eigenfunctions for G and J are mixed at H and K and then exchanged at I and L.

with e_c the eccentricity at the center of the avoided crossing. By using this relative deformation parameter, we can compare the results for various systems with different deformation parameters.

Shannon entropy of the probability density is numerically calculated for a closed elliptic billiard as a function of χ_e, and the result is shown in Fig. 2(a). The filled red-inverted (black-noninverted) triangles represent Shannon entropy for a red-dashed (black-dotted) A-B-C (D-E-F) trajectory of the eigenvalues in Fig. 1(a). We notice that the A-B-C trajectory has larger values of Shannon entropy than the D-E-F trajectory, but both of them change little as the eccentricity is varied. This result is no surprise since both probability densities remain almost unchanged as the eccentricity is varied, and the probability densities of the eigenfunctions on the D-E-F trajectory exhibit a smaller number of antinodes than those on the A-B-C trajectory.

Likewise, we can have the Shannon entropy of the probability density for an open elliptic billiard $S(\rho_k^{\mathrm{oe}}(r_i))$ with a similar normalization condition to that of the closed elliptic billiard. For the open elliptic billiard considered in Fig. 1(b), Shannon entropy is numerically calculated and the result is shown in Fig. 2(b) as a function of the relative deformation parameter χ_e. The unfilled red-inverted (black-noninverted) triangles represent Shannon entropy for a red-dashed (black-dotted) G-H-I (J-K-L) trajectory of the eigenvalues in Fig. 1(b). It is noted that the behavior of Shannon entropy of the probability density for the open elliptic billiard is quite different from that for the closed one. The Shannon entropy values of two eigenstates in the open elliptic billiard are maximized at the center of the avoided crossing. Moreover, they are exchanged across the avoided crossing. The Shannon entropy (unfilled black-noninverted triangles) associated with the eigenstate on the J-K-L trajectory is larger than that (unfilled red-inverted triangles) on the G-H-I trajectory for the negative relative deformation parameter $\chi_e \sim -0.06$. However, after going through the center of the avoided crossing, the Shannon entropy denoted by the unfilled black-noninverted triangles becomes smaller than that represented by the unfilled red-inverted triangles for the positive relative deformation parameter $\chi_e \sim 0.06$. This exchange of Shannon entropy is consistent with the pattern exchange of the eigenfunction intensity shown in Fig. 1(b).

It should be noted that the collective Lamb shift becomes dominant over the self-energy for large eccentricity in an open elliptic billiard, as shown in Fig. 1(b), resulting in an avoided crossing. At the avoided crossing, two interacting eigenfunctions are mixed together, resulting in more uniform probability distributions and consequently increased Shannon entropy, as shown in Fig. 2(b).

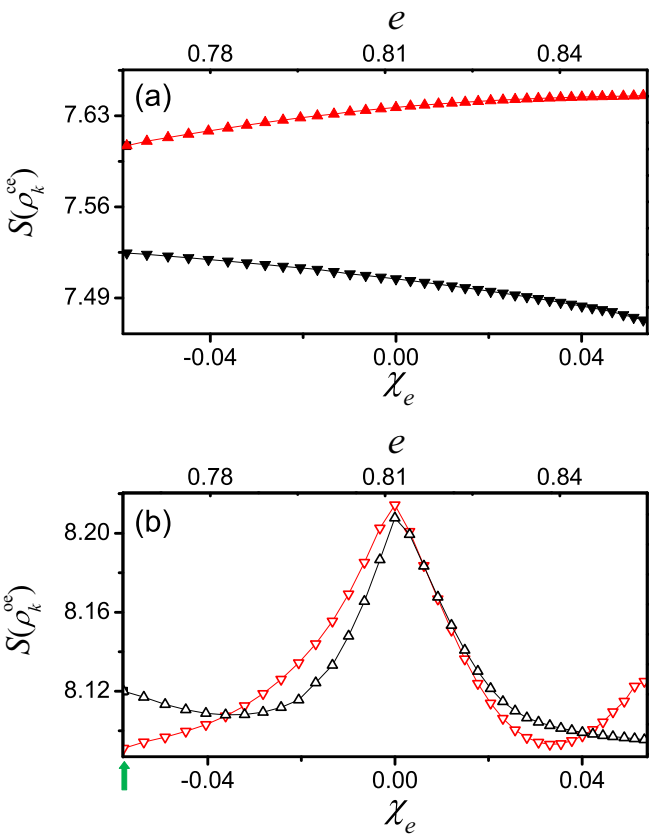

FIG. 2. Shannon entropy of the probability density for elliptic quantum billiards as a function of relative deformation parameter χ_e. (a) Shannon entropy for the closed elliptic billiard in Fig. 1(a). The filled red-inverted (black-noninverted) triangles represent Shannon entropy for the red-dashed (black-dotted) A-B-C (D-E-F) trajectory of the eigenvalues in Fig. 1(a). (b) Shannon entropy for the open elliptic billiard in Fig. 1(b). The unfilled red-inverted (black-noninverted) triangles represent Shannon entropy for the red-dashed (black-dotted) G-H-I (J-K-L) trajectory of the eigenvalues in Fig. 1(b). The thick green arrow indicates the deformation at which Shannon entropy values are listed in Sec. V.

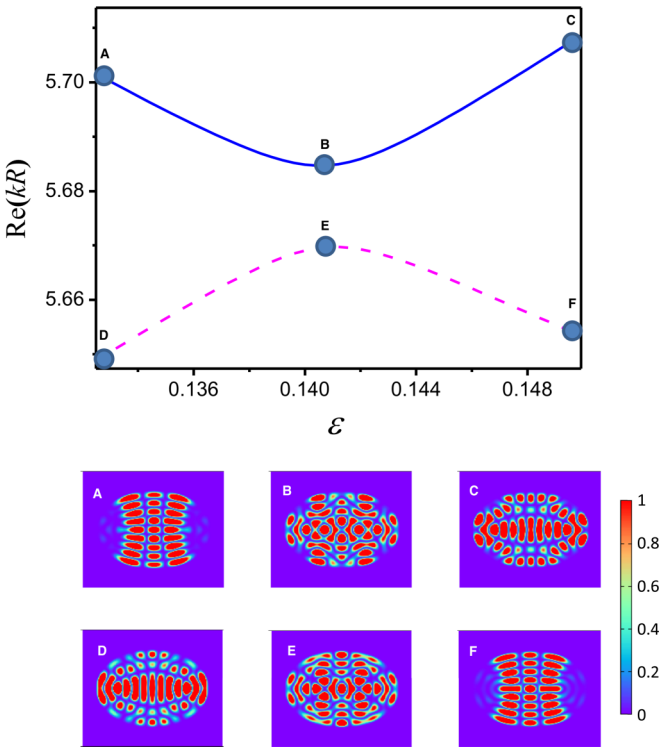

FIG. 3. The trajectories of eigenvalues and the intensities of some representative eigenfunctions in a closed quadrupole billiard. The upper panel shows the trajectories of eigenvalues with the deformation parameter ε. The avoided crossing takes place near $\varepsilon \simeq 0.141$. The lower panel shows that the eigenfunctions for A and D are mixed together at B and E, and then undergo mode exchange at C and F.

IV. SHANNON ENTROPY IN CLOSED QUADRUPOLE BILLIARDS

In this section, we consider a closed chaotic billiard. In particular, we consider a closed quadrupole described by $\rho(r) = 1 + \varepsilon\cos(2\phi)$ with a deformation parameter ε in the polar coordinates (r,ϕ). The eigenvalues λ_k and eigenfunctions $\psi_k^{cq}(\mathbf{r})$ are numerically calculated by using BEM [48] with an interval of $\Delta\varepsilon = 10^{-5}$. The superscript "cq" stands for "closed quadrupole." We consider TM modes with the Dirichlet boundary condition. The resulting trajectories of eigenvalues and the intensities of some of the eigenfunctions are shown in Fig. 3 as ε is varied from 0.132 to 0.149. It is seen that an avoided crossing takes place near $\varepsilon \cong 0.141$ as in an open elliptic billiard even though their origins are completely different from each other, as already discussed in Sec. II. Two distinct eigenfunctions at A and D are mixed together at B and E and then undergo a mode exchange at C and F. This type of avoided crossing is due to the symmetry breaking in a block-diagonal Hamiltonian for a closed quantum chaotic system. It is seen that the probability distributions of the mixed eigenfunctions at B and E reveal more uniform patterns than the unmixed ones at A, D, C, and F. Note that $\psi_k^{cq}(\mathbf{r})$ describing a chaotic system cannot form a complete basis set [20,21].

Figure 4 shows the Shannon entropy $S(\rho_k^{cq}(r_i))$ of the probability density for the closed quadrupole quantum billiard with a similar normalization condition to that of the closed elliptic billiard. The Shannon entropy is displayed as a function of the relative deformation parameter χ_ε defined as $\chi_\varepsilon = \frac{\varepsilon-\varepsilon_c}{\varepsilon}$ in the same way as χ_e in Eq. (5), with ε_c the deformation parameter at the center of the avoided crossing. We can thus compare the results of Figs. 2(b) and 4 with the same relative deformation parameter. The blue circles (magenta squares) represent Shannon entropy for the blue solid (magenta dashed) eigenvalue trajectory in Fig. 3. The Shannon entropies are maximized near the center of the avoided crossing ($\chi_\varepsilon \simeq 0.0$) and they are exchanged across the avoided crossing, similar to the Shannon entropies in the open elliptic billiard in Fig. 2(b).

V. MAXIMAL ENTROPY STATE AND EFFECT OF SELF ENERGY

Figures 2(b) and 4 show similar behaviors, that is, Shannon entropy is maximized as the center of avoided crossing is approached and they are exchanged across the avoided crossing in both cases. These similar behaviors come from the coherent superposition of wave functions in avoided crossings. However, the detailed behaviors are slightly different from each

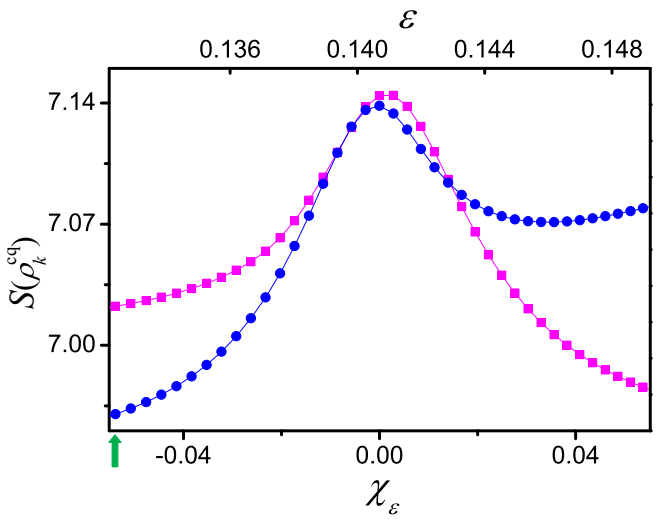

FIG. 4. Shannon entropy in a closed quadrupole quantum billiard as a function of the relative deformation parameter χ_ε. The blue circles (magenta squares) represent Shannon entropy for the blue solid (magenta dashed) eigenvalue trajectory in Fig. 3. Shannon entropy is maximized near the center of the avoided crossing, and they are exchanged across the avoided crossing. The thick green arrow indicates the deformation at which Shannon entropy values are listed in Sec. V.

other. The relative difference between two curves away from the center of avoided crossing in Fig. 2(b) is small (∼0.03) compared to that (∼0.06) in Fig. 4, and the behaviors of two curves in Fig. 2(b) are more complicated (curves cross each other three times) than those in Fig. 4. We suggest that these slightly different behaviors are due to the mode decay (self-energy), not the avoided crossing. To check this suggestion, let us consider a maximal entropy state and the self-energy.

A uniform probability distribution $q(x) = \frac{1}{N}$ for N states is a special one since it gives rise to maximal Shannon entropy, i.e., $S(\rho_{\max}) = \log N$. This maximal entropy can be obtained in a quantum billiard by identifying the number of states N with mesh points for numerical calculation of the system. The maximum entropy for the same number of mesh points ($N = 4166$) as used in Fig. 2 is $S(\rho_{\max}) \simeq 8.381$. Note that the states for the maximal entropy are not eigenstates of the Hamiltonian: we artificially impose uniform intensities in billiard systems. Obviously, if the mesh point N is fixed as a constant value, the maximal entropy is also fixed regardless of the deformation parameter.

To examine the self-energy (mode decay) effect on Shannon entropy, let us pay attention to the Shannon entropies at relative deformation parameter $\chi_e \cong -0.058$ indicated by thick green arrows in Figs. 2(a) and 2(b), well before the avoided crossing. They are denoted as $S_1^{(ce)}$ (red-inverted triangle) and $S_2^{(ce)}$ (black triangle) for the closed elliptical billiard, and $S_1^{(oe)}$ (open red-inverted triangle) and $S_2^{(oe)}$ (open black triangle) for the open elliptical billiard, respectively. The self-energy (mode decay) in an open system is an interaction with the bath itself, and it changes the boundary condition on billiards such that the wave functions at the boundaries are zero in closed billiards [Fig. 1(a)] whereas they are nonzero in open billiards [Fig. 1(b)]. This fact indicates that the self-energy Lamb shift makes the wave functions themselves dispersed simultaneously, making them closer to the maximal entropy state since the maximal entropy state corresponds to the completely dispersed state. As a result, the absolute values of Shannon entropy for wave functions in an open billiard become larger than those in a corresponding closed billiard. At the same time, the relative difference $\Delta S^{(oe)} = |S_2^{(oe)} - S_1^{(oe)}|$ between the two values of Shannon entropy in the open billiard becomes smaller than that in the closed billiard. Specifically, we have $S(\rho_{\max}) - S_1^{(oe)} = 0.289$, $S(\rho_{\max}) - S_2^{(oe)} = 0.261$, and thus $\Delta S^{(oe)} = 0.028$. Similarly for the closed elliptical billiard, we have $S(\rho_{\max}) - S_1^{(ce)} = 0.857$ and $S(\rho_{\max}) - S_2^{(ce)} = 0.774$, yielding $\Delta S^{(ce)} = 0.083$, much larger than that of the open elliptical billiard. A similar trend is observed with the closed quadrupole billiard, where $\Delta S^{(cq)} = 0.062$ at $\chi_\varepsilon \cong -0.058$, also much larger than that of the equally deformed open elliptical billiard. This fact implies that not only the collective Lamb shift but also the self-energy can induce a change in Shannon entropy. For these reasons, the detailed behaviors of Fig. 2(b) for an open billiard are different from those of Fig. 4 for a closed billiard. Since we focus on the relation between the avoided crossing and Shannon entropy in this paper, the detailed analysis on the self-energy effect on Shannon entropy will be discussed elsewhere.

VI. CONCLUSION

We investigated the relation between Shannon entropy and avoided crossings under strong coupling in dielectric microcavities. Before our work, the relation between Shannon entropy and avoided crossing was investigated in atomic physics, and the result was opposite to ours, i.e., Shannon entropy for an electron *decreases* due to electron ionization as we move close to the center of the avoided crossing. On the contrary, Shannon entropy of the probability density for dielectric microcavities (quantum billiards) *increases* due to the coherent superposition of wave functions as the center of the avoided crossing is approached, but both cases show exchanges of Shannon entropy as well as mode exchanges. Shannon entropy of the probability density for a closed elliptic billiard changes little with the eccentricity, while Shannon entropy of the probability density for an open elliptic billiard is maximized at the center of the avoided crossing. This maximization and exchange of Shannon entropy in an open elliptic billiard comes from the collective Lamb shift, which is an energy-level shift due to the interaction of energy levels with each other via the bath, and it can also induce an avoided crossing and coherent superposition of wave functions. In a closed quadrupole billiard, Shannon entropy is also maximized as the center of the avoided crossing is approached with both exchange of Shannon entropies as well as mode patterns. This maximization and exchange of Shannon entropy in a closed quadrupole billiard comes from the nonlinear dynamical effects in a chaotic system. Irrespective of the origin of the avoided crossings, the open elliptic cavity and the closed quadrupole cavity show similar behaviors to Shannon entropy. That is, the collective Lamb shift of open quantum systems and the symmetry breaking in the closed chaotic quantum systems have equivalent effects on the Shannon entropy.

ACKNOWLEDGMENTS

We thank M.-W. Kim and S. Rim for useful comments. This work was supported by the Korea Research Foundation (Grant No. 2016R1D1A109918326). K.J. acknowledges financial support by the Korea Research Foundation (Grants No. 2017R1E1A1A03070510 and No. 2017R1A5A1015626).

[1] C. E. Shannon, Bell Syst. Tech. J. **27**, 379 (1948).
[2] A. Hertz, M. G. Jabbour, and N. J. Cerf, J. Phys. A **50**, 385301 (2017).
[3] I. Bialynicki-Birula and J. Mycielski, Commun. Math. Phys. **44**, 129 (1975).
[4] W. H. Zurek, Rev. Mod. Phys. **75**, 715 (2003).
[5] S. Luo, Phys. Rev. A **77**, 042303 (2008).
[6] S. Fuhrman, M. J. Cunningham, X. Wen, G. Zweiger, J. J. Seilhamer, and R. Somogyi, BioSystem **55**, 5 (2000).
[7] F. L. Stahura, J. W. Godden, L. Xue, and J. Bajorath, J. Chem. Inf. Comput. Sci. **40**, 1245 (2000).
[8] N. Eagle, M. Macy, and R. Claxton, Science **328**, 1029 (2010).
[9] X. Zhang, N. Feng, Y. Wang, and Y. Shen, J. Sound Vib. **339**, 419 (2015).
[10] R. González-Férez and J. S. Dehesa, Phys. Rev. Lett. **91**, 113001 (2003).
[11] Y. L. He, Y. Chen, J. N. Han, Z. B. Zhu, G. X. Xiang, H. D. Liu, B. H. Ma, and D. C. He, Eur. Phys. J. D **69**, 283 (2015).
[12] J. von Neumann and E. Wigner, Physik. Z. **30**, 467 (1929).
[13] M. Christenen, A. B. Abrahamsen, N. B. Christensen, F. Juranyi, N. H. Andersen, K. Lefmann, J. Andreasson, C. R. H. Bahl, and B. B. Iversen, Nature Materials **7**, 811 (2008).
[14] M. Aizenman, P. Smeyers, and A. Weigert, A&A **58**, 41 (1997).
[15] A. M. F. Lau and C. K. Rhodes, Phys. Rev. A **16**, 2392 (1977).
[16] E. A. Cornell, R. M. Weisskoff, K. R. Boyce, and D. E. Pritchard, Phys. Rev. A **41**, 312 (1990).
[17] F. J. Arranz, L. Seidel, C. G. Giralda, R. M. Benito, and F. Borondo, Phys. Rev. E **82**, 026201 (2010).
[18] F. J. Arranz, F. Borondo, and R. M. Benito, Phys. Rev. Lett. **80**, 944 (1998).
[19] J. Wiersig, Phys. Rev. Lett. **97**, 253901 (2006).
[20] H.-J. Stöckmann, *Quantum Chaos: An Introduction* (Cambridge University Press, London, 1999).
[21] F. Haake, *Quantum Signatures of Chaos* (Springer, Berlin, 2010).
[22] I. Rotter, J. Phys. A: Math. Theor. **42**, 153001 (2009).
[23] F. M. Dittes, Phys. Rep. **339**, 215 (2000).
[24] K.-W. Park, J. Kim, and K. Jeong, Phys. Rev. A **94**, 033833 (2016).
[25] C.-H. Yi, H.-H. Yu, J.-W. Lee, and C.-M. Kim, Phys. Rev. E **91**, 042903 (2015).
[26] W. D. Heiss and A. L. Sannino, J. Phys. A **23**, 1167 (1990).
[27] Y. Shin, H. Kwak, S. Moon, S.-B. Lee, J. Yang, and K. An, Sci. Rep. **6**, 38826 (2016).
[28] S.-B. Lee, J. Yang, S. Moon, S.-Y. Lee, J.-B. Shim, S. W. Kim, J.-H. Lee, and K. An, Phys. Rev. Lett. **103**, 134101 (2009).
[29] S.-Y. Lee, J.-W. Ryu, J.-B. Shim, S.-B. Lee, S. W. Kim, and K. An, Phys. Rev. A **78**, 015805 (2008).
[30] S. Bittner, B. Dietz, H. L. Harney, M. Miski-Oglu, A. Richter, and F. Schäfer, Phys. Rev. E **89**, 032909 (2014).
[31] B. Dietz, T. Friedrich, J. Metz, M. Miski-Oglu, A. Richter, F. Schäfer, and C. A. Stafford, Phys. Rev. E **75**, 027201 (2007).
[32] J.-W. Ryu, S.-Y. Lee, and S. W. Kim, Phys. Rev. A **79**, 053858 (2009).
[33] Q. Song, Z. Gu, S. Liu, and S. Xiao, Sci. Rep. **4**, 4858 (2014).
[34] Q. Song, L. Ge, J. Wiersig, and H. Cao, Phys. Rev. A **88**, 023834 (2013).
[35] S.-B. Lee, J. Yang, S. Moon, S.-Y. Lee, J.-B. Shim, S. W. Kim, J.-H. Lee, and K. An, Phys. Rev. A **80**, 011802 (2009).
[36] R. K. Chang and A. J. Campillo, *Optical Processes in Microcavities* (World Scientific, Singapore, 1996).
[37] H. Feshbach, Ann. Phys. **5**, 357 (1958).
[38] N. Moiseyev, *Non-Hermitian Quantum Mechanics* (Cambridge University Press, Cambridge, 2011).
[39] E. Persson, I. Rotter, H.-J. Stöckmann, and M. Barth, Phys. Rev. Lett. **85**, 2478 (2000).
[40] G. L. Celardo and L. Kaplan, Phys. Rev. B **79**, 155108 (2009).
[41] K.-W. Park, J. Kim, and K. Jeong, Opt. Commun. **368**, 190 (2016).
[42] I. Rotter, Fortschr. Phys. **61**, 178 (2013).
[43] E. J. Heller, Phys. Rev. Lett. **53**, 1515 (1984).
[44] S. Fishman, D. R. Grempel, and R. E. Prange, Phys. Rev. Lett. **49**, 509 (1982).
[45] M. C. Gutzwiller, J. Math. Phys. **12**, 343 (1971).
[46] O. Bohigas, M. J. Giannoni, and C. Schmit, Phys. Rev. Lett. **52**, 1 (1984).
[47] J. M. G. Gómez, K. Kar, V. K. B. Kota, R. A. Molina, A. Relaño, and J. Retamosa, Phys. Rep. **499**, 103 (2011).
[48] J. Wiersig, J. Opt. A **5**, 53 (2003).
[49] J.-H. Kim, J. Kim, C.-H. Yi, H.-H. Yu, J.-W. Lee, and C.-M. Kim, Phys. Rev. E **96**, 042205 (2017).